Image inpainting algorithm based on partial differential equation technique

Article *in* Imaging Science Journal The · March 2013

DOI: 10.1179/1743131X11Y.0000000055

2 authors:

Shuaijie Li
Henan University of Science and Technology
15 PUBLICATIONS **40** CITATIONS
SEE PROFILE

Zheng-an Yao
Sun Yat-Sen University
166 PUBLICATIONS **1,062** CITATIONS
SEE PROFILE

Image inpainting algorithm based on partial differential equation technique

S J Li* and **Z A Yao**
Department of Mathematics and Computational Science, Sun Yat-sen university, Guangzhou, 510275, China

Abstract: Image inpainting is the process of filling in missing parts of damaged images based on information gleaned from surrounding areas. In this paper, we present two variational models for image inpainting. Combining two models, we can simultaneously fill in missing, corrupted or undesirable information, while remove noise. We explain that diffusion performance of the proposed models is essentially superior to that of TV inpainting model by analysing the physical characteristics in local coordinates, and investigate the existence of minimising functionals in BV space. The experimental results show the effective performance of the proposed models in restoring scratched photos, text removal, and even removal of entire objects from images.

Keywords: image inpainting, variational approach, energy functional, PDEs

1 INTRODUCTION

Image inpainting is the filling in of damaged or missing parts of an image with the use of information from surrounding areas, and is a important task in image processing. In essence, it is a type of interpolation. Its applications include restoration of old paintings, removing scratches from old photographs, altering scenes in photographs and restoration of motion pictures.

The pioneering work of image inpainting was introduced into image processing by Bertalmio *et al.*[1] The most recent approaches to non-texture inpaingting are based on the partial differential equations (PDEs) and calculus of variations. In Ref. 1, their model was based on nonlinear PDEs, and was designed to imitate the techniques of museum artists who specialise in restoration. this idea was further extended to guarantee that the level curves are propagated into the inpainting domain. In subsequent work with Ballester *et al.*,[2] the authors proposed to minimise an energy to compute the restored image and this results in the solving of coupled nonlinear differential equations. In Ref. 3, a connection between the isophote direction of the image and the Navier–Stokes equation was observed and they proposed to solve transport equations to fill in the inpainting domain. Tai *et al.*[4] proposed a two-step method to do image inpainting. Firstly, the isophote directions for the missing regions by solving a nonlinear total variation (TV)-Stokes equation was constructed, then an image was restored to fit the constructed direction.

A different approach to inpainting was proposed by Chan and Shen.[5] They introduced the idea that well-known total variational image denoising models[6] can be easily adapted to the inpainting task by a simple modification. In later work,[7–9] energy involving the curvature of the level curves was used and this was in some sense trying to guarantee that the level curves were connected in a smooth fashion. The equations obtained from such models were highly nonlinear and of higher (fourth) order. Following in

The MS was accepted for publication on 17 November 2011.
* *Corresponding author: Shuaijie Li, Department of Mathematics and Computational Science, Sun Yat-sen university, Guangzhou, 510275, China; email: ls-jie@163.com*

 IMAG 282 © RPS 2013 DOI: 10.1179/1743131X11Y.0000000055

the footsteps of Chan and Shen, Esedoglu and Shen[10] adapted the Mumford–Shah image segmentation model[11] to the inpainting problem for greyscale image, and Grossauer and Scherzer[12] used the complex Ginzburg–Landau equation in a technique for inpainting problem of greyscale images. More recently, a fast non-iterative method for image inpainting was proposed based on first-order transport equation,[13] which traversed the inpainting domain by the fast marching method just once while transporting along the way; image values in a coherence direction robustly were estimated by means of the structure tensor.

On the other hand, texture inpainting has attracted attention. In Ref. 14, the image in the surrounding area was first decomposed into texture and structure and then propagated into the inpainting domain in different ways. This idea to decompose texture and structure was also used in Ref. 15. Some statistical approaches were used in Refs. 16–20 to do texture synthesis and structure propagation. In Refs. 17 and 18, the authors proposed to add spatial coherence in the texture synthesis process. These so-called exemplar-based approaches proposed in Refs. 19 and 20 were non-local: to determine the value at each point, the whole image might be scanned in the search for a matching patch.

The idea used in this work is motivated by Chan *et al.*[5,7,8] We still follow the basic ideas of variational models of image inpainting, i.e. we are trying to implement image inpainting by minimising energy functional. Compared with other inpainting schemes, the TV model[5,7,8] has the lowest complexity and easiest digital implementation. It works remarkably well for local inpainting such as scratches and text removal. But for large-scale inpainting, the TV inpainting model suffers from its origin in the length curve energy. The major drawback of the TV model is that it does not restore satisfactorily a single object when the disconnected remaining parts are separated far apart by the inpainting domain[18] and introduce staircase effect when filling in large smooth domain.[19]

In this paper, we propose two new variational image inpainting models based on a energy functional depending on whether or not noise needs to be suppressed in the image. We adopt different diffusion processes for the image, whether it contains noise or not. The basic idea of our algorithm is to complete these regions which hold no information and eliminate noise (if exists) while preserving the edges and avoiding staircase effect.

The outline of the paper is as follows. In Section 2, we will briefly review the TV inpainting model. And we will propose two new models for image inpainting in Section 3, and analyse the models and present the existence theorems of the models in Section 4. Section 5 discusses some numerical implementation issues, and shows experiments and analysis. Conclusion is drawn in the last sections.

2 TV INPAINTING MODEL

In this section, we recall the TV inpainting model[5] in brief. Assume that u_0 is contaminated by homogeneous white noise. The variational inpainting model is to find a function u on the whole domain Ω, such that it minimises an appropriate regularity functional

$$\Phi(u)=\int_{\Omega}\phi(|\nabla u|)\mathrm{d}x \tag{1}$$

under the fitting (or denoising) constrain on D^{C}

$$\frac{1}{|D^{\mathrm{C}}|}\int_{\mathrm{D^C}}|u-u_0|^2\mathrm{d}x=\sigma^2 \tag{2}$$

Here ϕ: $R\rightarrow R$ is an increasing function which governs the regularisation behaviour according to the gradient magnitude $|\nabla u|$, and σ is the standard deviation of the white noise. D denotes the inpainting domain, and $D^{\mathrm{C}}=\Omega\backslash D$ is the available domain. As in the TV restoration model of Rudin, Osher and Fatemi,[6] Chan solved the unconstrained TV inpainting problem

$$J_{\lambda}(u)=\int_{\Omega}|\nabla u|\mathrm{d}x+\frac{\lambda}{2}\int_{\mathrm{D^C}}|u-u_0|^2\mathrm{d}x \tag{3}$$

where λ plays a role of the Lagrange multiplier for the constrained variational problem (equations (1) and (2)). The Euler–Lagrange equation for the energy functional J_{λ} is

$$-\nabla\cdot\left(\frac{\nabla u}{|\nabla u|}\right)+\lambda_{\mathrm{D^C}}(u-u_0)=0,\quad x\in\Omega \tag{4}$$

and plus the Neumann boundary condition. Here the extended Lagrange multiplier λ_{D} is given by

$$\lambda_{\mathrm{D^C}}(x)=\begin{cases}\lambda, & x\in D^{\mathrm{C}}\\ 0, & x\in D\end{cases} \tag{5}$$

The infinitesimal steepest descent equation for $J_{\lambda}(u)$ is therefore given by

$$\frac{\partial u}{\partial t}=\nabla\cdot\left(\frac{\nabla u}{|\nabla u|}\right)+\lambda_{\mathrm{D^C}}(u_0-u) \tag{6}$$

Since λ_{D^C} takes two different values, the problem is a two-phase problem, and the interface is the boundary of inpainting domain.

3 THE PROPOSED INPAINTING MODEL

In order to propose our inpainting model, a general variational inpainting model can be written as

$$J_\lambda(u)=\int_\Omega \phi(|\nabla u|)\mathrm{d}x+\frac{\lambda}{2}\int_{D^C}|u-u_0|^2\mathrm{d}x \tag{7}$$

There are various researches by choosing a proper ϕ to propose certain local behavior. If choosing $\phi(s)=s$, that leads to the TV inpainting model. As we know, the benefit of TV model is that it preserves edges, thus making significant features easily identifiable. However, TV model may mistake noise as a significant feature, thus creating unwanted artifacts or false edges. Costanzino[21] chooses $\phi(s)=s^2$ that leads to the well-known harmonic model. The main benefit of harmonic model is that it removes noise, but it has a major drawback in that significant feature such as edges are not preserved.

In order to carry out anisotropic diffusion on the edges and inpainting domain and isotropic diffusion in regular regions, it is well known[22] that the function ϕ should satisfy

$$\begin{cases}\phi'(0)=0,\ \lim\limits_{s\to 0^+}\phi''(s)=\lim\limits_{s\to 0^+}\dfrac{\phi'(s)}{s}=c>0\\ \lim\limits_{s\to\infty}\phi''(s)=\lim\limits_{s\to\infty}\dfrac{\phi'(s)}{s}=0,\ \lim\limits_{s\to\infty}\dfrac{s\phi''(s)}{\phi'(s)}=0\end{cases} \tag{8}$$

In this work, we choose $\phi(s)=s\log(1+s)$, apparently, $\phi(s)=s\log(1+s)$ satisfies the hypothesis (8). With these factors, we propose two variational models for image inpainting.

Model I (noise free inpainting model): If the original image is free noise, or the noise is small enough to be negligible, one just needs to fill in the damaged domains and preserve the other undamaged domains. We propose a simple energy minimisation scheme to fill in the missing parts.

$$J^1(u)=\int_\Omega |\nabla u|\log(1+|\nabla u|)\mathrm{d}x,\quad u|_{D^C}=u_0|_{D^C} \tag{9}$$

Model II (noisy inpainting model): Another important issue of inpainting is how to deal with noise, since in applications, the left part of the image $u_0|_{D^C}$ is often noisy. So the constraint condition in equation (9) is replaced by the denoising one (equation (2)). So we propose noisy inpainting model:

$$J^2(u)=\int_\Omega |\nabla u|\log(1+|\nabla u|)\mathrm{d}x+\frac{\lambda}{2}\int_{D^C}|u-u_0|^2\mathrm{d}x \tag{10}$$

Minimising the energy functional $J^1(u)$ and $J^2(u)$ about u, we can get the Euler–Lagrange equations for the energy function $J^1(u)$ and $J^2(u)$:

$$-\nabla\cdot\left\{\left[\frac{\log(1+|\nabla u|)}{|\nabla u|}+\frac{1}{1+|\nabla u|}\right]\nabla u\right\}=0 \tag{11}$$

$$-\nabla\cdot\left\{\left[\frac{\log(1+|\nabla u|)}{|\nabla u|}+\frac{1}{1+|\nabla u|}\right]\nabla u\right\}+\lambda_{D^C}(u-u_0)=0 \tag{12}$$

The steepest descent equation for $J^1(u)$ and $J^2(u)$ are given by

$$\begin{cases}u_t=\nabla\cdot\left\{\left[\dfrac{\log(1+|\nabla u|)}{|\nabla u|}+\dfrac{1}{1+|\nabla u|}\right]\nabla u\right\}, & \text{in } D\\ u=u_0, & \text{on } \partial D\\ u|_{t=0}=u_0, & \text{in } \overline{D}\end{cases} \tag{13}$$

and

$$\begin{cases}u_t=\nabla\cdot\left\{\left[\dfrac{\log(1+|\nabla u|)}{|\nabla u|}+\dfrac{1}{1+|\nabla u|}\right]\nabla u\right\}+\lambda_{D^C}(u_0-u), & \text{in } \Omega\\ \dfrac{\partial u}{\partial \vec{n}}=0, & \text{on } \partial\Omega\\ u|_{t=0}=u_0, & \text{in } \overline{\Omega}\end{cases} \tag{14}$$

where $\vec{n}$ is the unit out normal vector of Ω. The existence and uniqueness of weak solutions for the nonlinear parabolic equations (13) and (14) has been established in Refs. 23–26.

4 ANALYSIS OF THE MODELS

4.1 Existence theorems

Theorem 1 (Existence of Model I): Suppose that the original image $u_0 \in BV(\Omega)$and $0\leqslant u_0\leqslant 1$, then the minimising problem $\min\limits_u J^1(u)$ has at least solution $u \in BV(\Omega)$.

Proof Since the original complete image u_0 is admissible, we can always find a minimising sequence u_n for the model. Then both

$$\int_\Omega |\nabla u_n|\mathrm{d}x \quad\text{and}\quad \int_\Omega |u_n|\mathrm{d}x \tag{15}$$

are bounded for all n since Ω is bounded and u_n takes values in the greyscale interval [0, 1]. By the weak compactness property of BV functions, there is a subsequence, still denoted by u_n for convenience,

which strongly converges to some $u \in L^1(\Omega)$in the L^1 norm. Apparently u still meets the constraints

$$u|_{D^C} = u_0|_{D^C} \quad \text{and} \quad u(x) \in [0, 1] \tag{16}$$

By the lower semi-continuity property of BV space and property of the convex function

$$\int_\Omega |\nabla u| \log(1+|\nabla u|) \leq \lim_{n \to +\infty} \inf \int_\Omega |\nabla u_n| \log(1+|\nabla u_n|) \tag{17}$$

Thus, u must be a minimiser.

Theorem 2 (Existence of Model II): Suppose that the original image $u_0 \in BV(D^C) \bigcap L^2(D^C)$ and $0 \leqslant u_0 \leqslant 1$, then the minimising problem $\min_u J^2(u)$ has at least solution $u \in BV(\Omega)$.

Proof We observe $u_0 \in BV(D^C) \bigcap L^2(D^C)$, and define $\overline{u}_0$ by extending u_0 by 0 in D. Then $\overline{u}_0 \in [0, 1]$, and $\overline{u}_0 \in BV(\Omega) \bigcap L^2(\Omega)$. There exists a minimising sequence of admissible inpainting $\{u_n\}$. Thanks to the greyscale constraint, $\{u_n\}$ must be bounded in $BV(\Omega)$. Thus, there is subsequence, still denoted by $\{u_n\}$ for convenience, which converges in L^1 norm to some $u \in L^1(\Omega)$. By the lower semi-continuity property of BV space and property of the convex function

$$\int_\Omega |\nabla u| \log(1+|\nabla u|) \leq \lim_{n \to +\infty} \inf \int_\Omega |\nabla u_n| \log(1+|\nabla u_n|) \tag{18}$$

We can further refine the subsequence so that

$$u_n \to u, \quad \text{a·e· on } \Omega \tag{19}$$

Thus, u must meet the greyscale constraint, and more importantly, by the Lebesgue Dominated Convergence Theorem

$$\int_{D^C} (u-u_0)^2 dx = \lim_{n \to +\infty} \int_{D^C} (u_n-u_0)^2 dx \tag{20}$$

Therefore, u is a minimiser of $J^2(u)$.

4.2 Performance of diffusion

In the following, we analyses the physical performance of equations (13) and (14). We are going to show that it can be decomposed using the local image structures. Choose a local orthogonal coordinate system (ξ,η), such that the η-axis is parallel to the gradient direction at a point and the ξ-axis is perpendicular, i.e.

$$\xi = \frac{1}{|\nabla u|}(-u_y, u_x) = \frac{\nabla^\perp u}{|\nabla u|}, \; \eta = \frac{1}{|\nabla u|}(u_x, u_y) = \frac{\nabla u}{|\nabla u|} \tag{21}$$

That is, in the local coordinates (ξ,η), equation (13) can rewrite as

$$u_t = T(|\nabla u|) u_{\xi\xi} + N(|\nabla u|) u_{\eta\eta} \tag{22}$$

where $T(|\nabla u|) = \dfrac{\log(1+|\nabla u|)}{|\nabla u|} + \dfrac{1}{1+|\nabla u|}$ and $N(|\nabla u|) = \dfrac{1}{1+|\nabla u|} + \dfrac{1}{(1+|\nabla u|)^2}$

From equation (22), the coefficients T and N controlled the diffusion performance of equation (13) in the gradient direction and the isophote direction. Now we consider two limit situations $|\nabla u| \to 0$ and $|\nabla u| \to \infty$ in the following.

1. When $|\nabla u| \to 0$, $\lim_{|\nabla u| \to 0} T(|\nabla u|) = \lim_{|\nabla u| \to 0} N(|\nabla u|) = 2$. Because the diffusion coefficients are the same, equation (13) is essentially isotropic diffusion equation. It can propagate the information into the inpainting domain along the isophote direction and the gradient direction.
2. When $|\nabla u| \to \infty$, $\lim_{|\nabla u| \to \infty} [N(|\nabla u|)/T(|\nabla u|)] = 0$. It indicates that the diffusion performance in isophote direction is much stronger than the one in the gradient direction. There is hardly diffusion in the gradient direction, so the equation is essential anisotropic diffusion equation, and mainly transport the information from the surrounding inpainting domain into its interior always following the isophote direction.

According to the above analysis, for image inpainting, we can propagate the information into the inpainting domain along the isophote and gradient direction when surrounding inpainting domain is smooth, but only in the isophote direction when surrounding inpainting domain is edge. Secondly, for image denoising, we assure that the proposed model can avoid the staircase effect in smooth region, while it can still keep the sharp edges effectively.

5 NUMERICAL IMPLEMENTATION AND EXPERIMENTAL RESULTS

In the section, we show the numerical results by applying the proposed models on images of varying difficulty. Firstly, we present numerical implementation about the proposed models. Then, we approximate the problem (14) by an semi-implicit finite difference scheme:

$$u_{i,j}^{k+1} = u_{i,j}^k + \Delta t \left\{ \nabla \cdot \left[F(u^k) \nabla u^{k+1} \right]_{i,j} + \lambda_{D^C} (u_0 - u^{k+1})_{i,j} \right\} \tag{23}$$

where $F(u^k) = \log(1+|\nabla u^k|)/|\nabla u^k| + 1/(1+|\nabla u^k|)$, and Δt denotes time step. More precisely, the degenerate

1 Inpainting results. The first column is original images, the second column is damaged images, and the last two columns are inpainting results by TV inpainting model and the proposed model, respectively

diffusion term $\nabla\cdot\left[F(u^{k})\nabla u^{k+1}\right]_{i,j}$ can be approximated by a standard five-point finite difference scheme

$$\begin{aligned}\nabla\cdot\left[F(u^{k})\nabla u^{k+1}\right]_{i,j}=&(D_{i+1/2,j}+D_{i,j+1/2}+D_{i-1/2,j}+D_{i,j-1/2})u_{i,j}^{k+1}\\&-(D_{i+1/2,j}u_{i+1,j}^{k+1}+D_{i-1/2,j}u_{i-1,j}^{k+1}+\\&D_{i,j+1/2}u_{i,j+1}^{k+1}+D_{i,j-1/2}u_{i,j-1}^{k+1})\end{aligned}\tag{24}$$

where

$$D_{i+1/2,j}=F(u_{i+1,j}^{k}-u_{i,j}^{k})\tag{25}$$

and the same structures are taken for $D_{i-1/2,j}$, $D_{i,j+1/2}$ and $D_{i,j-1/2}$. The iterative equation (23) can be quickly implemented using additive operator splitting method.[27–29] For equation (13), it is similar to implement using the above method.

Next, we compare the inpainting performance of the TV inpainting model and the proposed model in the work on the same images, and we adopt additive operator splitting method for both models. Then we will show some inpainting results of the proposed model in practical applications. In order to objectively testing the performance of image inpainting, we will use the improved of signal-to-noise ratio (ISNR) that is defined as

$$\mathrm{ISNR}=10\log_{10}\frac{\|I_0-I\|_{L^2}}{\|I_0-I_{\mathrm{new}}\|_{L^2}}$$

where I_0, I and I_{new} are original image, damaged image and reconstructed image, respectively.

In Fig. 1, we illustrate the effect of TV inpainting model and the proposed model I to damaged images but no noise. The first column is original images, the second column is damaged images and the last two

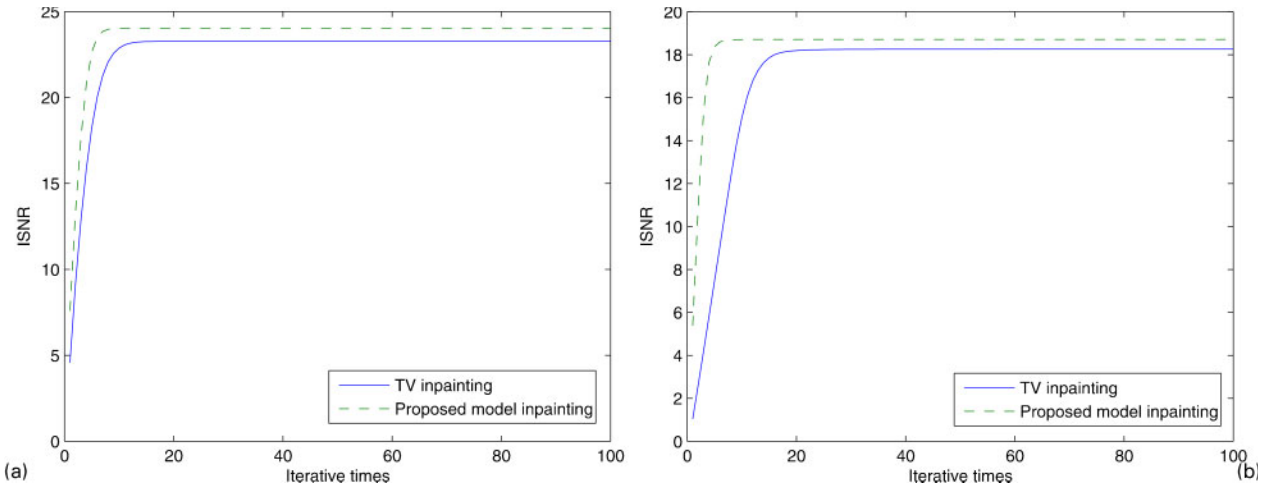

2 Comparisons of TV inpainting model and the proposed model about ISNR: (a) Barbara; (b) Cameraman

3 Inpainting results. The first column is original images; the second column is damaged images and the last two columns are inpainting results by TV inpainting model and the proposed model, respectively.

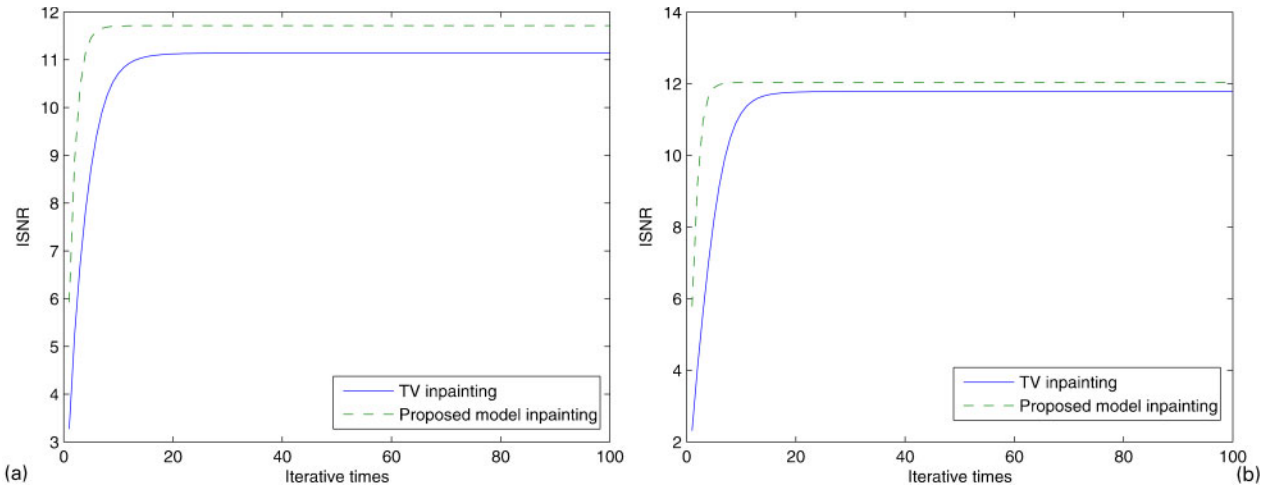

4 Comparisons of TV inpainting model and the proposed model about ISNR: (a) Lena; (b) Pepper

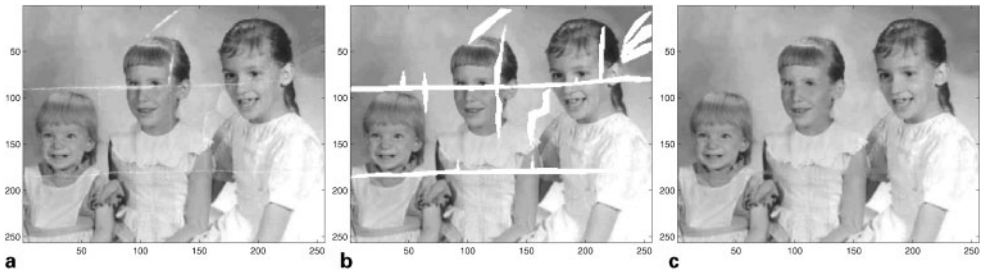

5 Inpainting results: (a) the original image; (b) the image with the inpainting region in white; (c) the restored image

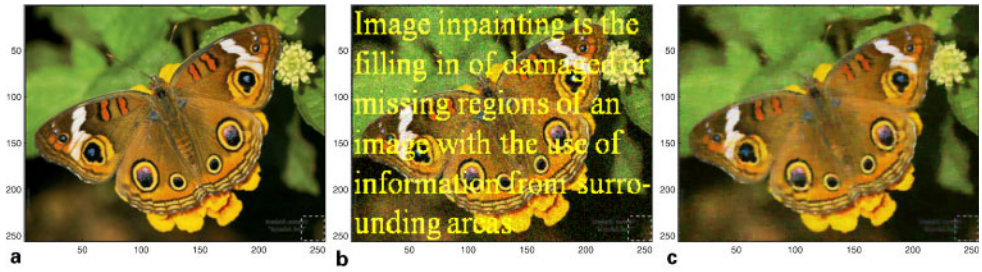

6 Inpainting results: (a) the original image; (b) the damaged image; (c) the restored image

columns are inpainting results by TV inpainting model and the proposed model I, respectively. The results show that inpainting performance of both models is as good as desired. Figure 2 shows the relationship between ISNR and iterative times in experiments. From Fig. 2, we can see that the algorithms have reach steady state at 20 times, and the proposed model has better performance in convergence speed and inpainting quality. Iterations were performed with time step $\Delta t=10$ and iterative times $k=100$.

The second example is showed in Figs. 3 and 4. In Fig. 3, the first column is original images that are damaged by scratches, characters and noise as shown in the second column, and the last two columns are inpainting results by TV inpainting model and the proposed model II, respectively. Our proposed model is better than the TV inpainting model both in performance and in efficiency (Figs. 3 and 4), because our proposed model can remove the scratches, characters and noise, and avoid staircase effect. The used parameters were $\Delta t=10$, $k=100$ and $\lambda=0.1$.

We test our model on a well-known example which has been tested by others using different methods.[2] We use these results to show the quality of the restored images. Figure 5 shows an old photo which has been damaged. We mark the inpainting region in white colour, as shown in Fig. 5b, and try to restore it. The result is shown in Fig. 5c. With Model I, iterations were performed with time step $\Delta t=10$ and iterative times $k=40$.

In the next example shown in Fig. 6, the image is corrupted by yellow text and Gaussian noise. The text is the inpainting domain, and we want to fill it with information from the image. The other is denoising area, and we should remove noise. With Model II, $\Delta t=10$, $\lambda=0.1$ and iterative times $k=40$, we can get this result as shown in Fig. 6c.

In the last two example, we want to remove the unwanted objects and restore the landscape in the background. Figure 7a is the original picture and Fig. 7b–h shows how the eagle is gradually disappearing during the iterations. Similar to Fig. 7, in

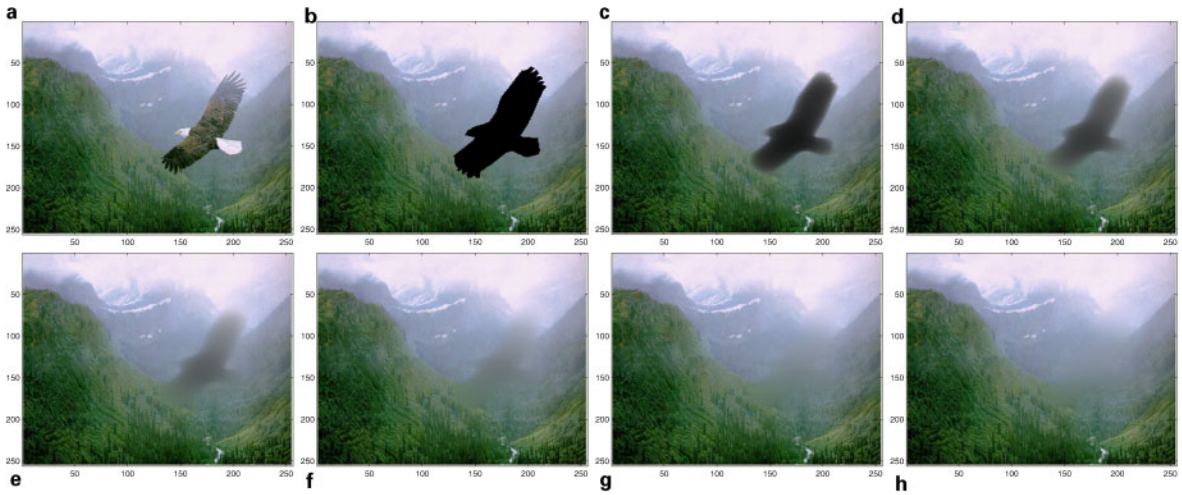

7 Inpainting results: (a) the original image; (b) the image with the inpainting region in black; (c) at iteration 20; (d) at iteration 40; (e) at iteration 60; (f) at iteration 80; (g) at iteration 100; (h) the final image with iterative 150

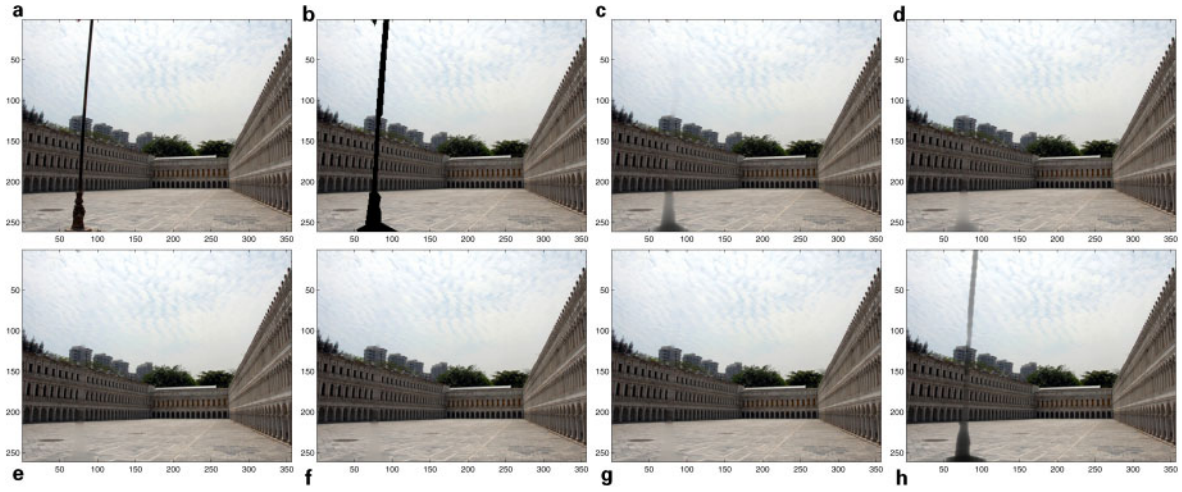

8 Inpainting results: (a) the original image; (b) the image with the inpainting region in black; (c) at iteration 10; (d) at iteration 20; (e) at iteration 40; (f) at iteration 60; (g) at iteration 80; (h) the final image with iterative 100

Fig. 8, we show that lamppost is gradually removed and get the perfect landscape.

6 CONCLUSION

In this paper, depending on whether or not noise needs to be removed in the image, we present two mathematical models for image restoration, which consist of the recovery of missing parts in an image and also removing the corruption caused by noise.

The two models presented in this work are inspired on the TV inpainting model for image restoration. Corrupted by missing information and noise, the restoration is carried out by a adaptive equation, which performs diffusion outside of the inpainting domain and transportation inside of the inpainting domain. Corrupted by missing information or covered by text or other objects, the restoration is carried by transporting data to the inpainting domain.

We have analysed the physical characteristics of the related parabolic equations in local coordinates and explain that diffusion performance is essentially superior to that of TV inpainting model. The results showed in our examples also demonstrate the high performance of the proposed models which have demonstrated better efficiency than TV inpainting model in dealing with the inpainting of damaged images (Figs 1 and 5) or denoising when the initial image is noisy (Fig. 3 and 6), and made a better general performance in convergence speed and inpainting quality as one can see in Figs. 2 and 4.

ACKNOWLEDGEMENTS

The authors would like to thank National Nature Science Foundation of China (No.10971234), Tianyuan Foundation of National Nature Science Foundation of China (No.11026227), Fundamental Research Funds for the Central Universities (No.10lgzd09), and Technology Plan Funds of Guangzhou (No.2010C6-I00011).

REFERENCES

1 Bertalmio, M., Sapiro, G., Ballester, C. and Caselles, V. In Proceedings of SIGGRAPH 2000: Computer Graphics Annual Conference Series (Ed. K. Akeley), 2000, pp. 417–424 (ACM Press/ACM SIGGRAPH/ Addison Wesley Longman, New York).

2 Ballester, C., Bertalmio, M., Caselles, V., Sapiro, G. and Verdera, J. Filling in by joint interpolation of vector fields and gray levels. *IEEE Trans. Image Process.*, 2001, **10**, 1200–1211.

3 Bertalmio, M., Bertozzi, A. L. and Sapiro, G. Navier–Stokes, fluid dynamics and image and video inpainting. *IEEE Comput. Vis. Patt. Recogn.*, 2001, **1**, 355–362.

4 Tai, X. C., Osher, S. and Holm, R. In Image Processing Based on Partial Differential Equations, 2006, pp. 3–33 (Springer, Heidelberg).

5 Chan, T. F. and Shen, J. Mathematical models for local non-texture inpaintings. *SIAM J. Appl. Math.*, 2002, **62**, 1019–1043.

6 Rudin, L., Osher, S. and Fatemi, E. Nonlinear total variation based noise removal algorithms. *Physica D*, 1992, **60**, 259–268.

7 Chan, T. F., Kang, S. H. and Shen, J. Euler: elastica and curvature-based inpainting. *SIAM J. Appl. Math*., 2002, **63**, 564–592.

8 Chan, T. F., Shen, J. and Vese, L. Variational PDE models in image processing. *Not. Am. Math. Soc*., 2003, **50**, 14–26.

9 Chan, T. F. and Shen, J. Non-texture inpainting by curvature-driven diffusions (CDD). *J. Vis. Commun. Image Represent*., 2001, **12**, (4), 436–449.

10 Esedoglu, S. and Shen, J. Digital inpainting based on the Mumford–Shah–Euler image model. *Eur. J. Appl. Math*., 2002, **13**, 353–370,.

11 Mumford, D. and Shah, J. Optimal approximations by piecewise smooth functions and associated variational problems. *Commun. Pure Appl. Math*., 1989, **42**, 577–685.

12 Grossauer, H. and Scherzer, O. Using the complex Ginzburg–Landau equation for digital inpainting in 2D and 3D. *Lect. Notes Comput. Sci*., 2003, **2695**, 225–236.

13 Bornemann, F. and März, T. Fast image inpainting based on coherence transport. *J. Math. Imaging Vis*., 2007, **28**, 259–278.

14 Bertalmio, M., Vese, L., Sapiro, G. and Osher, S. Simultaneous texture and structure image inpainting. *IEEE Trans. Image Process*., 2003, **12**, 882–889.

15 Elad, M., Starck, J., Querre, P., Donoho, D. Simultaneous cartoon and texture image inpainting using morphological component analysis (MCA). *Appl. Comput. Harmon. Anal*., 2005, **19**, 340–358.

16 Criminisi, A., Perez, P. and Toyama, K. Region filling and object removal by exemplar-based image inpainting. *IEEE Trans. Image Process*., 2004, **13**, 1200–1212.

17 Wexler, Y., Shechtman, E. and Irani, M. Space–time video completion. *IEEE Trans. Pattern Anal. Mach. Intell*., 2007, **29**, 1463–1476.

18 Fadili, M., Starck, J. and Murtagh, F. Inpainting and zooming using sparse representations. *Comput. J*., 2009, **52**, 64–79.

19 Komodakis, N. and Tziritas, G. Image completion using efficient belief propagation via priority scheduling and dynamic pruning. *IEEE Trans. Image Process*., 2007, **16**, 2649–2661.

20 Aujol, J., Ladjal, S. and Masnou, S. Exemplar-based inpainting from a variational point of view. *SIAM J. Math. Anal*., 2010, **42**, 1246–1285.

21 Costanzino, N. *Structure Inpainting via Variational Methods* [online], 2002 (Providence, RI, LEMS). Available at: <http://www.lems.brown.edu/~nc/> Accessed 6 October 2011.

22 Aubert, G. and Kornprobst, P. Mathematical Problems in Image Processing, 2002 (Springer-Verlag, Berlin).

23 Wang, L. H. and Zhou, S. L. Existence and uniqueness of weak solutions for a nonlinear parabolic equation related to image analysis. *J. Part. Differ. Equ*., 2006, **19**, 97–112.

24 Huang, H., Jia, C. and Huan, Z. On weak solutions for an image denoising-deblurring model. *Appl. Math. J. Chin. Univ*., 2009, **24**, 269–281.

25 Feng, Z. and Yin, Z. On the weak solutions for a class of nonlinear parabolic equations related to image analysis. *Nonlinear Anal.: Theory Methods Appl*., 2009, **71**, 2506–2517.

26 Feng, Z. and Yin, Z. Weak solutions for a class of generalized nonlinear parabolic equations related to image analysis. *J. Math. Anal. Appl*., 2010, **368**, 235–246.

27 Tai, X. Global extrapolation with a parallel splitting method. *Numer. Algorithm*, 1991, **3**, 527–440.

28 Weickert, J., ter haar Romeny, B. M. and Viergever, M. A. Efficient and reliable schemes for nonlinear diffusion filtering. *IEEE Trans. Image Process*., 1998, **7**, 398–410.

29 Kuhne, G., Weickert, J., Viergever, M. and Effelsberg, W. Fast implicit activ coutour models. *Lect. Notes Comput. Sci*., 2002, **2449**, 133–140.